Int J Ind Chem (2017) 8:207–220
DOI 10.1007/s40090-016-0109-5

RESEARCH

Adsorption and desorption kinetics of toxic organic and inorganic ions using an indigenous biomass: *Terminalia ivorensis* seed waste

Jonathan O. Babalola[3] · Funmilayo T. Olayiwola[3] · Joshua O. Olowoyo[3] · Alimoh H. Alabi[3] · Emmanuel I. Unuabonah[2] · Augustine E. Ofomaja[1] · Martins O. Omorogie[1,2]

Received: 30 April 2016 / Accepted: 11 December 2016 / Published online: 23 December 2016

Abstract Environmental remediation has been a strategy employed by scientists to combat water pollution problems that have led to the scarcity of potable water. Hence, in this study, *Terminalia ivorensis* seed waste (TISW) was explored for the removal of Congo Red, Methylene Blue, Cadmium and Lead from aqueous solutions. Some experimental variables such as pH, biosorbent dose, initial solute ion concentration, agitation time and temperature were optimised. The surface microstructures of TISW were studied using proximate analysis, bulk density, specific surface area, pH of Point of Zero Charge, Fourier Transform Infra Red Spectroscopy, Thermogravimetric/Differential Thermal Analysis, Scanning Electron Microscopy and Energy Dispersive Analysis of X-ray. The maximum Langmuir monolayer saturation adsorption capacity, $q_{\max_L}$, was obtained as 175.44 mg/g for the removal of Methylene Blue by TISW. Also, the $q_{\max_L}$ for CR, Cd(II) ion and Pb(II) ion were 85.47, 12.58 and 52.97 mg/g, respectively. Also, the pseudo-first-order constant, k_1, and pseudo-second-order rate constant, k_2, are 0.008–0.026 min^{-1} and 0.012–0.417 mg g^{-1} min^{-1}, respectively. Hence, TISW is recommended as a good adsorbent for the removal of both toxic industrial dyes and toxic metal ions from polluted water.

Keywords *Terminalia ivorensis* · Thermodynamics · Kinetics · Mass transfer · Desorption

Introduction

The quest for potable water has been a serious challenge to the global ecological balance, especially in developed countries. The recent interest in water shortage and water pollution has driven researchers very hard, so as to look for a lasting, effective and efficient solution to this menace combating the survival of human lives and the ecology. Today, 800 million people still lack access to potable water. For instance, only 46% of the Oceania population and 39% of the Sub-Sahara Africa population have access to potable water [1–4]. The sporadic rise in human activities over the decades has led to the consistent release of various recalcitrant anthropogenic pollutants into water bodies, thereby causing a sharp drop in the quality of the ecosystem. Eradication of these deleterious pollutants is difficult using classical water purification systems. Report from the World Health Organisation (WHO) showed that 1.8 million people die from polluted water-related diseases [2]. In Nigeria, this problem aggravates the sustainability of its ecology, leading to the precarious survival of flora and fauna. Hence, this has heralded an urgent need for researchers to proffer a sustainable solution to this life quagmire [5–8]. Toxic metals are known to be the most

Electronic supplementary material The online version of this article (doi:10.1007/s40090-016-0109-5) contains supplementary material, which is available to authorized users.

✉ Jonathan O. Babalola
bamijibabalola@yahoo.co.uk

✉ Martins O. Omorogie
omorogiem@run.edu.ng;
osaigbovooohireimen@gmail.com; martinso@vut.ac.za

[1] Adsorption and Catalysis Research Laboratory, Department of Chemistry, Vaal University of Technology, Private Bag X021, Andries Potgieter Boulevard, Vanderbijlpark 1900, South Africa

[2] Environmental and Chemical Processes Research Laboratory, Department of Chemical Sciences, Redeemer's University, P.M.B. 230, Ede, Osun State, Nigeria

[3] Department of Chemistry, University of Ibadan, 200284 Ibadan, Nigeria

problematic pollutants, due to their non-biodegradable nature. Irrespective of the huge effort that has been put together by researchers to minimise their environmental impact, toxic metals in the environment still have adverse effects on human, fauna and flora. The toxicological effects of Cd(II) and Pb(II) in humans include bone lesions, cancers (kidney and lung), hypertension, inhibition of haemoglobin formation, sterility, infants brain impairment, learning disabilities, abortion, and kidney damage. To date, various remediation technologies have been used to treat polluted water containing toxic synthetic dyes and metals. These are coagulation, chemical oxidation, photodegradation, aerobic or anaerobic oxidation, precipitation, membrane filtration, dialysis, ion exchange, solvent extraction, reverse osmosis, among others [9, 10]. These technologies have some drawbacks, such as low selectivity, incomplete removal, cost ineffectiveness and production of large amount of secondary sludge. Adsorption is known as a green, sustainable and cost-effective technology, which is an alternative to other remediation technologies mentioned above. In recent times, natural or modified biomaterials (biosorbents and agricultural byproducts), which comprise lignin, cellulose, hemicelluloses and other organic compounds that have various functional moieties, have been found to be ubiquitous, easily sourced, cheap, green, sustainable and good adsorbents for clean recovery of toxic synthetic dyes and metals [9]. Some researchers in their previous treatises have used eucalyptus seeds [9], peanut hulls [11], corn cob [12], almond shell, hazelnut shell [13], olive cake [14], mungbean husk [15], mango peel waste [16], orange waste [17], *Scolymus hispanicus L.* [18], chemically modified orange peel [19], *Nauclea diderrichii* seed biomass [20, 21], *Zea mays* seed chaff [22], Mesoporous SiO_2/-graphene oxide nanoparticles-modified *Nauclea diderrichii* seed biomass [23, 24], *Parkia biglobosa* biomass [25], *Papaya*-clay combo [26], MnO_2 nanoparticles-modified *Nauclea diderrichii* biomass waste [27], TiO_2 nanoparticles-modified *Nauclea diderrichii* seed biomass [28], *Pentaclethra macrophylla* and *Malacantha alnifolia* barks [29]. Other researchers in the literature used other adsorbent and techniques to treat wastewaters in addition to adsorption [30–53].

Terminalia ivorensis, a timber tree, is the sole member of the genus that occurs naturally in West Africa. It is an indigenous plant (family *Combretaceae*) which is recognised in the South-western rain forest of Nigeria and Ghana. The bark is used as a lotion for the treatment of wounds, sores and cuts. *Terminalia ivorensis* is a large deciduous forest tree. On plantations, weeding up to the second year and line cleaning or creeper cutting from the third to sixth year may be necessary. With the diverse native uses of this species, its utility can be further enhanced for agroforestry development by the present research effort on it [54]. *Terminalia ivorensis* is found in the rainforest but is predominantly a tree of seasonal forest zones. *Terminalia ivorensis* has numerous uses in the building, construction, carpentry industries and household equipment. Also, this plant can also use as ethnomedicine, a lotion for the treatment of wounds, sores and cuts because it healed without scar [54].

The seed epicarp of *Terminalia ivorensis* is initially removed before the seed is planted. This seed epicarp constitutes a colossal amount of obnoxious waste. This has informed our choice of exploring this waste as a biosorbent for this research. Conventional remediation technologies like coagulation, membrane filtration, dialysis, reverse osmosis, etc., utilized to treat water polluted with toxic metal ions and dyes are very expensive and result in secondary pollution. The use of *Terminalia ivorensis* seed waste will avail researchers and industries the opportunity to substitute the aforementioned cocktails of conventional technologies above with very cheap, convenient, suitable, eco-friendly and secondary pollution-free technology to treat polluted water.

This work explores the remediation potential of green, sustainable, cost-effective, ubiquitous, and locally sourced biomass of *Terminalia ivorensis* seed waste (TISW) for some toxic pollutants studied. To the best of the authors' knowledge, TISW is a new biological adsorbent which is reported to have good uptake capacities for MB, CR, Cd(II) and Pb(II).

Experimental

Preparation of *Terminalia ivorensis* seed waste (TISW)

Terminalia ivorensis seed waste (TISW) was obtained from the Forest Research Institute of Nigeria (FRIN), in Ibadan (7°23′16″ North, 3°53′47″ East), Nigeria. After collection, it was air dried for four weeks and later oven dried for 22 h at 70 °C. The dried bark was cut into small pieces and pulverised. Further drying was carried out for 6 h. The pulverised TISW was sieved to 250 µm, put into plastic containers and used for various adsorption experiments.

Surface microstructures of TISW

Proximate analysis, bulk density, pH of point of zero charge (PZC), specific surface area (SSA), Fourier transform infra red spectroscopy (FTIR), thermogravimetric/differential thermal analysis (TG/DTA), scanning electron microscopy (SEM) and energy dispersive analysis of X-ray (EDAX) of TISW

Proximate analysis and bulk density of TISW were determined according to the published protocol of Ofomaja and

Naidoo [55]. The pH of point zero charge of TISW was determined according to the published protocol of Stumm and Morgan [56]. The specific surface area of TISW was determined according to the published protocol of Sears [57]. The Fourier Transform Infra Red spectroscopic analyses of unloaded, and toxic metals/dyes loaded TISW were carried out by Perkin Elmer FTIR Spectrophotometer (Spectrum Version 2) at the scanning frequencies of 400–4000 cm^{-1}. The Perkin Elmer thermogravimetric/differential thermal analysis (TG/DTA) was carried out by Perkin Elmer TG/DTA thermal analyser. Furthermore, the surface microstructures of TISW were carried out by Scanning Electron Microscopy (SEM) instrument, coupled with Energy Dispersive Analysis of X-ray (EDAX), JEOL JSM-6390 LV Model.

All the experimental details and mathematical equations used for these adsorption and desorption studies are shown in the Electronic Supporting Information (ESI) of this manuscript.

Results and discussion

Surface characterization of TISW microstructures

Proximate analysis, bulk density, PZC, SSA, FTIR, TG/DTA, SEM and EDAX of TISW

The percentage proximate compositions of TISW on dry weight basis are depicted in Table 1. The determined bulk density of TISW was 0.05 g cm^{-3}. The SSA of TISW was 240.6 m^2 g^{-1}. The PZC of the TISW was 6.44.

The PZC or (isoelectric pH) of biosorbent is the pH at which the density of anionic moieties is equal to that of the cationic moieties on a biosorbent surface. At pH < PZC, the surface of a biosorbent is predominantly cationic, while at pH > PZC, its surface is predominantly anionic. The functional moieties on TISW surface probably acquire negative or positive charges depending on the solution pH [55]. The PZC result of TISW suggests that it possesses a broad solution pH range to retain its positive charges (see Fig. 1).

The FTIR spectra of TISW, with its loaded CR, MB, Pb^{2+} and Cd^{2+} analogues are shown in figures S1a-S1e of the ESI. The free O–H stretch for TISW appeared at 3871 and 3748 cm^{-1}. After loading TISW with CR, MB and Pb^{2+}, there was no shift in the vibration frequency of the free O–H stretch. For Cd^{2+}-loaded TISW, the vibration frequency shifted to 3759 cm^{-1}. The N–H stretch of TISW was observed at 3456 cm^{-1}. The N–H stretch for CR, MB, Pb^{2+} and Cd^{2+}-loaded TISW shifted to 3445, 3438, 3447 and 3443 cm^{-1}, respectively. These shifts in the vibration frequencies might be due to binding of these toxic ions onto the functional moieties in the cell walls of TISW [29]. The C–H of CH_2 and CH_3 for TISW was observed at 2935 cm^{-1}. No significant shift was observed for MB, Pb^{2+} and Cd^{2+}-loaded TISW. But for CR-loaded TISW, the C-H vibration frequency decreased to 2924 cm^{-1}. The –C=O stretch for TISW was found at 1648 cm^{-1}. For MB-loaded TISW, the vibration frequency decreased 1623 cm^{-1}. There were negligible shifts in the vibration frequency of –C=O stretch for TISW loaded with CR, Pb^{2+} and Cd^{2+}. The aromatic –C=C– stretch for TISW appeared at 1544 cm^{-1}. Also, there was no significant change in the –C=C– vibration frequency when TISW was loaded with CR, MB, Pb^{2+} and Cd^{2+}. The C–H bend for TISW appeared at 1359 cm^{-1}. This vibration frequency increased to 1376 and 1384 cm^{-1} for CR-loaded TISW, and Pb^{2+} and Cd^{2+}-loaded TISW. For MB-loaded TISW, this vibration frequency decreased to 1348 cm^{-1}. The –C–O bend for TISW was observed at 1057 cm^{-1}. However, there were negligible shifts in the vibration frequency of –C–O bend for TISW loaded with MB, CR, Pb^{2+} and Cd^{2+}. For TISW, the –C–O out of plane deformation bend was observed at 582 cm^{-1}. This vibration frequency shifted to 571 and 568 cm^{-1} for CR and MB-loaded TISW, and Pb^{2+} and Cd^{2+}-loaded TISW, respectively. The various shifts in the stretch and bend vibration frequencies after loading TISW with the studied pollutant ions/molecules might result from chelation, precipitation and ion exchange reactions that was involved in the biosorption process (see Table 2) [29].

The TG of TISW (see Fig. 2) showed that <220 °C, ca. 11% weight loss was observed due to the loss of surface water from TISW. At temperature >220 and <550 °C, ca. 55% weight loss was observed, which was assigned to the loss of the volatile components of lignocelluloses and hemicelluloses of TISW [20, 21]. Above 550 °C, TISW was thermally stable. For DTA (also see Fig. 2) of TISW, exothermic heat flow assigned to 1% decrease in derivative weight was observed from 33 to 150 °C, endothermic heat flow assigned to 1.5% increase in derivative weight was observed from >150 to 180 °C, another exothermic heat flow assigned to 5% decrease in derivative weight was observed from 180 to 350 °C and two endothermic heat flows assigned to 3.5 and 0.5% increases in derivative

Table 1 Proximate analysis of *Terminalia ivorensis* seed waste

% Moisture content	% Crude protein	% Crude fat	% Crude fibre	% Ash content
3.09	10.51	1.84	24.36	6.45

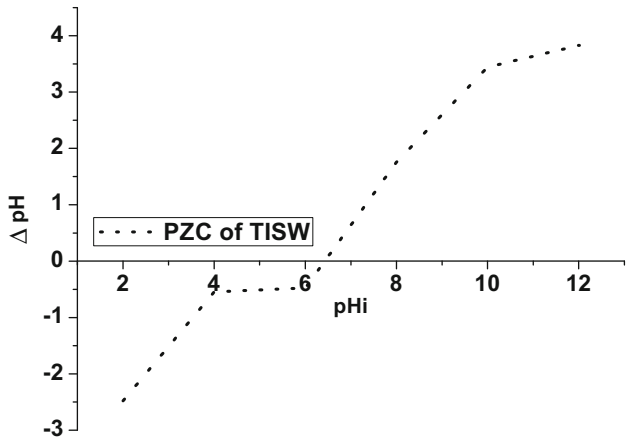

Fig. 1 The pH of point of zero charge plot for *Terminalia ivorensis* seed waste

weight were observed from >350 to 400 °C and 400 to 580 °C, respectively. The exothermic heat flows led to the dissociation of some chemical bonds of lignocelluloses and hemicelluloses of TISW. Also, the endothermic heat flows led to the association of some chemical bonds to form small molecules such as CO, CO_2, NH_3, etc. [20, 21, 25, 58].

The SEM micrographs of TISW show tiny irregular, scattered and spaced fibrils of the lignocelluloses that are contained in the cell walls that comprise lumped particles of unconnected and broken walls. The EDAX of TISW showed the elemental compositions of TISW, which was an indication of the constituents of the functional moieties in TISW (see Fig. 3a–d).

Influence of pH on the removal of sorbate ions onto TISW

The influence of solution pH on the biosorption capacity of TISW largely depends on the speciation of the sorbate or solute ions/molecules at different pHs of the aqueous solutions. The removals of CR and MB onto TISW were highest at pH 2.0 and pH 12.0, respectively. These were obtained as 3.34 and 12.36 mg/g, respectively. The biosorption of CR was optimum at pH 2.0 due to increase in the proton cloud densities of TISW (see Fig. 4). This enabled negatively charged CR molecules to bind easily to the surface of TISW. On the other hand, the removal of MB onto TISW was found to be optimum at pH 12.0 due to the low proton cloud densities on the surface of TISW. This accounted for the increase in the removal of positively charged MB molecules onto TISW [21, 29].

Furthermore, the removal of Cd^{2+} onto TISW was highest at pH 6.0. This was obtained at 10.60 mg/g. Also, >pH 7.0, there was a very slight increase in the removal of Cd^{2+} to 10.64 mg/g. The negatively charged

Table 2 Fourier transform infrared spectra characteristics of *Terminalia ivorensis* seed waste before and after biosorption of Methylene Blue, Congo Red, Cadmium and Lead

Dyes/metals	Absorption band peak (cm^{-1})			Functional groups
	Before	After	Difference	
CR	3871.14	3871.14	–	Free –OH
MB		3871.14	–	Free –OH
Pb(II)		3865.54	5.600	Free –OH
Cd(II)		3871.14	–	Free –OH
CR	3747.89	3742.29	5.600	Free –OH
MB		3747.89	–	Free –OH
Pb(II)		3742.29	5.600	Free –OH
Cd(II)		3759.10	11.21	Free –OH
CR	3456.00	3445.00	11.00	N–H Stretch
MB		3438.00	18.00	N–H Stretch
Pb(II)		3447.00	9.000	N–H Stretch
Cd(II)		3443.00	13.00	N–H Stretch
CR	2935.57	2924.36	11.21	C–H Stretch
MB		2929.97	5.600	C–H Stretch
Pb(II)		2929.97	5.600	C–H Stretch
Cd (II)		2935.57	–	C–H Stretch
CR	1648.20	1647.56	0.640	C=O—Stretch
MB		1623.00	25.20	C=O—Stretch
Pb(II)		1650.20	1.800	C=O—Stretch
Cd(II)		1645.00	3.200	C=O—Stretch
CR	1544.05	1538.46	5.590	Aromatic C=C
MB		1538.46	5.590	Aromatic C=C
Pb(II)		1538.46	5.590	Aromatic C=C
Cd(II)		1541.25	2.800	Aromatic C=C
CR	1359.44	1376.22	16.78	S=O—Stretch
MB		1348.25	11.19	S=O—Stretch
Pb(II)		1384.61	25.17	S=O—Stretch
Cd(II)		1384.61	25.17	S=O—Stretch
CR	1057.34	1054.54	2.800	C–O– Stretch
MB		1048.95	8.390	C–O—Stretch
Pb(II)		1051.74	5.600	C–O—Stretch
Cd(II)		1057.34	–	C–O—Stretch
CR	581.81	570.62	11.19	C–S—Stretch
MB		570.62	11.19	C–S—Stretch
Pb(II)		567.83	23.98	C–S—Stretch
Cd(II)		565.03	16.78	C–S—Stretch

TISW surface at weak acidic and neutral pH favoured the high uptake of Cd^{2+} due to deprotonation (low proton density). The very negligible increase for the removal of Cd^{2+} by TISW observed at >pH 6.0 might be due to the likelihood of the precipitation of Cd^{2+} on the functional sites on the cell walls of TISW. On the other hand, the removal of Pb^{2+} by TISW was highest at pH 6.0. This was obtained at 12.13 mg/g. At pH >6.0–7.0, Pb^{2+} no longer exists in the solution. The speciation of Pb^{2+} at this pH led

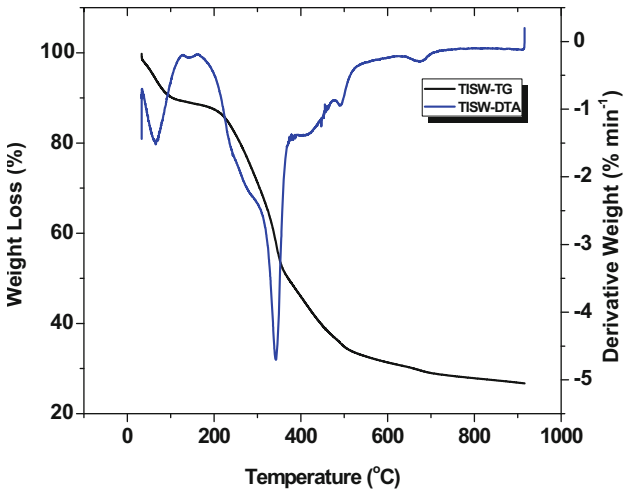

Fig. 2 Thermogravimetric/differential thermal analysis for *Terminalia ivorensis* seed waste

to the formation of $Pb(OH)^{+}$, $Pb(OH)_2$, $Pb(OH)_3^{-}$ and $Pb(OH)_4^{2-}$. From the PZC value of TISW, which was 6.44, it suggested that TISW retained positive charges on its surface over a pH range <6.44. Due to this, TISW would biosorbed high amount of CR molecules than the positive pollutant ions/molecules through ion exchange mechanism and electrostatic attraction. The adsorption of Pb^{2+} continued until precipitation occurred at pH >6.0. Hence, at pH >6.0–7.0, the binding of $Pb(OH)^{+}$ species to the TISW biosorbent surface occurred by complexation mechanism and, at this point, further biosorption of Pb^{2+} ceased. Hence, the main mechanisms by which MB and CR molecules interact with TISW were by electrostatic attraction and π–π hydrophobic interactions. These π–π hydrophobic interactions are higher in CR molecule than MB molecule due to the many aromatic rings in CR thus it has higher propensity to bind to the negatively charged

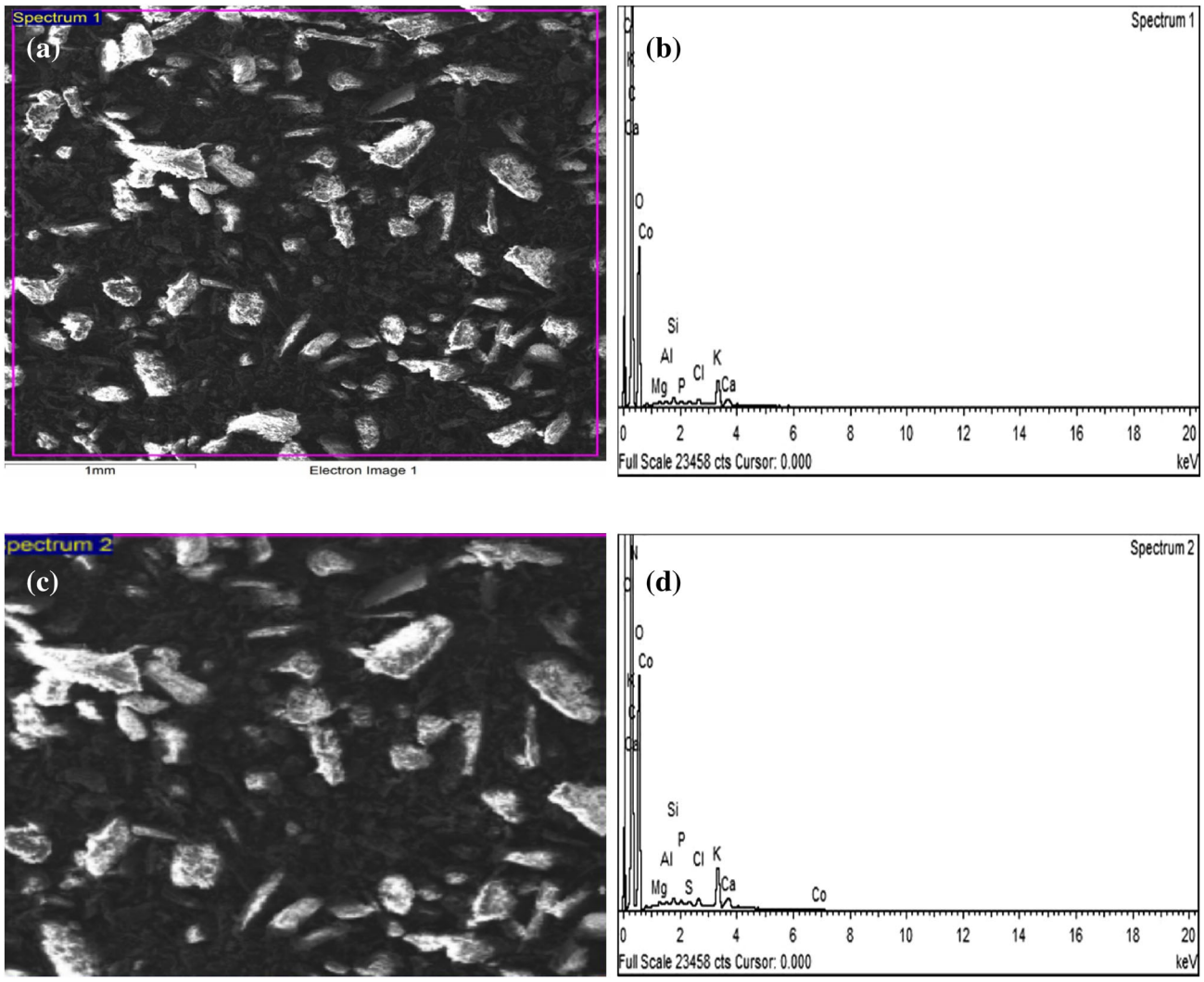

Fig. 3 **a–d** Scanning electron micrographs and energy dispersive analysis of X-ray for *Terminalia ivorensis* seed waste

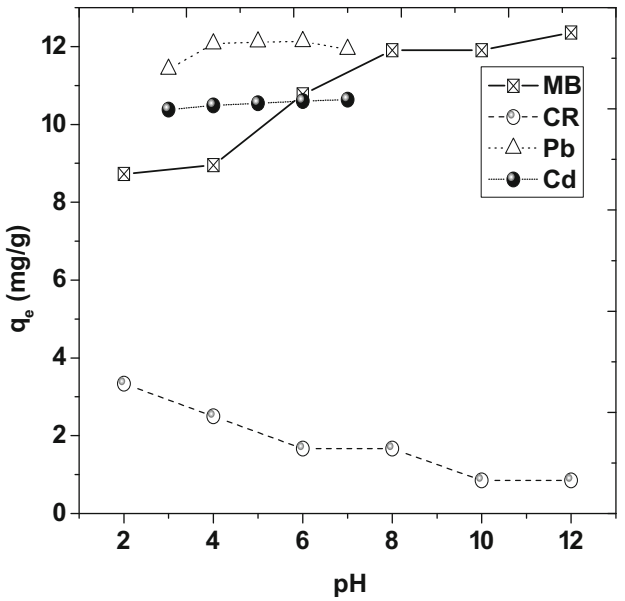

Fig. 4 The plots of the amounts of Methylene Blue, Congo Red, Cadmium and Lead biosorbed by *Terminalia ivorensis* seed waste, q_e (mg/g) against pH (pH 2.0–7.0 for Cadmium and Lead; pH 2.0–12.0 for Methylene Blue and Congo Red); adsorbent dose = 25 mg; agitation speed = 200 rpm; initial metal ion concentration = 100 mg/L; agitation time = 180 min; temperature = 300 K)

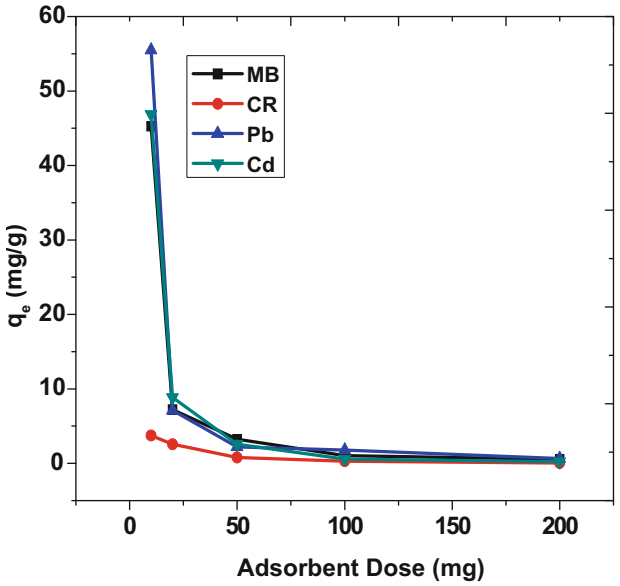

Fig. 5 The plots of the amounts of Methylene Blue, Congo Red, Cadmium and Lead biosorbed by *Terminalia ivorensis* seed waste, q_e (mg/g) against adsorbent dose (adsorbent dose = 10–200 mg; agitation speed = 200 rpm; initial metal ion concentration = 100 mg/L; agitation time = 180 min; temperature = 300 K)

functional moieties on the surface of TISW by π–π hydrophobic interactions than MB. Electrostatic attraction occurred when MB or CR molecules bound to the negatively charged functional moieties on the surface of TISW depending on the pH of the aqueous solutions. On the other hand, the main mechanisms for the uptake of Cd^{2+} and Pb^{2+} by TISW were by electrostatic attraction and complexation, which are dependent on the pH of the working solutions as expounded above [29].

Influence of adsorbent dose on the removal of sorbate ions onto TISW

The amount of sorbate ions biosorbed decreased with increase in biosorbent dose from 10 to 200 mg. This decrease became more pronounced as the weight of the biosorbent increased, resulting in the agglomeration or aggregation of biosorbent particles, probably blockage of biosorption sites, reduced surface area for sorbate–sorbent interaction and the lengthening of diffusion path [55]. Figure 5 shows the plots of the amount of solute ions adsorbed at equilibrium, q_e (mg/g) against adsorbent dose (mg).

Influence of initial sorbate ions concentration on the biosorption capacity of TISW

The initial sorbate ions concentration is a cogent factor that determines the mass transfer and diffusion dynamics of the biosorption of sorbate or solute ions onto biomasses. Also, increase in the initial sorbate ions concentration is the driving force that is needed to overcome the mass transfer resistance of the uptake of solute ions onto the surface of the biomass [59].

As the initial concentrations of CR and MB increased from 25 to 750 mg/L, there was a commensurate rise in their removal from 6.30 to 362.80 and 10.17 to 362.04 mg/g respectively. Also, the increase in the initial concentrations of Cd^{2+} and Pb^{2+} from 25 to 750 mg/L also amounted in the proportionate increase in Cd^{2+} and Pb^{2+} biosorbed by TISW from 11.55 to 146.89 and 10.48 to 176.22 mg/g, respectively. It is noteworthy to mention here that the increase in the initial concentration of sorbate ions led to the corresponding increase in their uptakes, as they occupied the functional moieties on the surface of TISW. The binding of these solute ions to these functional moieties in the active sites occurred in quick successions until they were occupied [25, 29].

Influence of agitation time on the removal of sorbate ions onto TISW

The residence time of solute ions plays a salient role in the solute ions uptake onto the biosorbent surface, due to its influence on the sorbent–solute interface. Ho [60] and Onal et al. [61] proposed that biosorption consists of three steps, which are: (a) the diffusion of adsorbate through the solution to the external surface of the adsorbent or the boundary layer

Table 3 Linear equilibrium parameters for the removal of Methylene Blue, Congo Red, Cadmium and Lead onto *Terminalia ivorensis* seed waste

	Langmuir model			Freundlich model			Temkin model		
	$q_{\max_L}$ (mg/g)	k_L (L/mg)	R^2	k_f $(L/mg)^{\frac{1}{n}}(mg/g)$	$1/n$	R^2	k_T (L/mg)	b_T	R^2
MB	175.44	0.05	0.99	0.15	2.41	0.95	6.23	12.46	0.83
CR	85.47	0.02	1.00	2.63	0.93	0.99	3.74	40.60	0.93
Cd(II)	12.58	0.04	0.99	14.79	0.43	0.78	3.03	70.60	0.66
Pb(II)	52.91	0.04	0.96	3.89	0.53	0.87	3.53	123.54	0.94

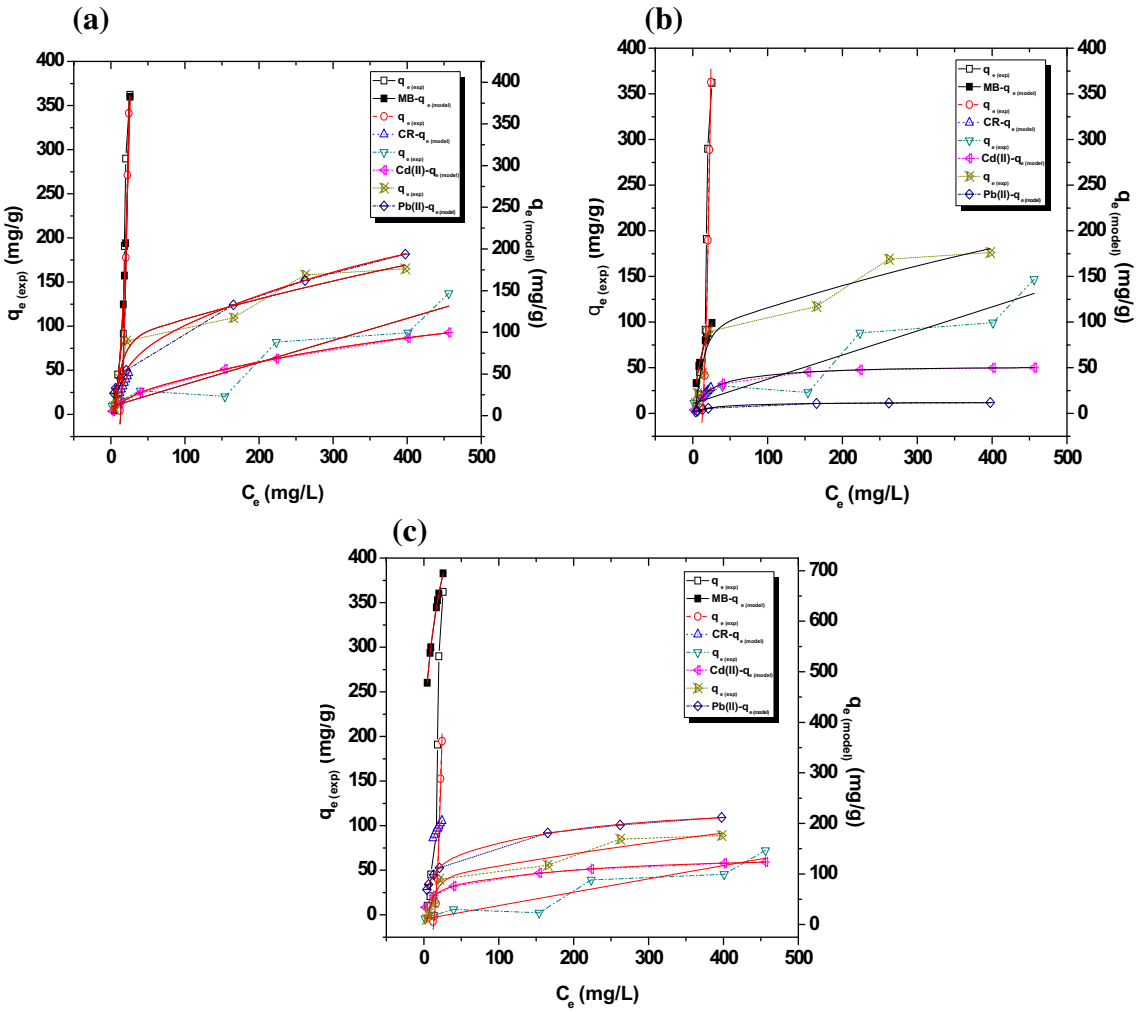

Fig. 6 **a** Nonlinear Freundlich isotherm plots of Methylene Blue, Congo Red, Cadmium and Lead biosorbed by *Terminalia ivorensis* seed waste (temperature = 300 K; adsorbent dose = 25 mg; agitation speed = 200 rpm; initial metal ion concentration = 25–500 mg/L; agitation time = 180 min). **b** Nonlinear Langmuir isotherm plots of Methylene Blue, Congo Red, Cadmium and Lead biosorbed by *Terminalia ivorensis* seed waste (temperature = 300 K; adsorbent dose = 25 mg; agitation speed = 200 rpm; initial metal ion concentration = 25–500 mg/L; agitation time = 180 min). **c** Nonlinear Temkin isotherm plots of Methylene Blue, Congo Red, Cadmium and Lead biosorbed by *Terminalia ivorensis* seed waste (temperature = 300 K; adsorbent dose = 25 mg; agitation speed = 200 rpm; initial metal ion concentration = 25–500 mg/L; agitation time = 180 min)

diffusion of the solute molecules, (b) the gradual adsorption step, in which intraparticle diffusion may be rate limiting and (c) the diffusion of adsorbate particles to adsorption sites either by pore diffusion through the liquid-filled pores or by a solid diffusion mechanism.

The biosorption of CR by TISW at temperature of 300 K increased up to 15 min. Thereafter, equilibrium was attained. Also, the biosorption of CR by TISW increased up to 30 and 60 min at 320 and 340 K respectively, after which equilibrium was reached. It could be said that

increase in temperature led to an increase in the time equilibrium was attained for the biosorption of CR onto TISW. At 300 K, CR molecules rapidly occupied the available functional moieties on the active sites in 15 min of biosorption process. At 320 and 340 K, the available functional moieties on the active sites were occupied at 30 and 60 min, respectively. Although, increase in the temperature from 300 to 340 K was meant to increase in the driving force (mass transfer) of CR molecules onto the functional moieties in the pores of TISW due to the increase in the collision frequency and mobility of CR molecules [29, 62]. This temperature increase might have led to the rupture of some chemical bonds of the functional moieties of TISW, distorting the π–π stacking from hydrophobic interactions of CR aromatic rings. Hence, this phenomenon decreased the propensity of CR molecules to bind to TISW surface [29]. The biosorption of MB onto TISW at 300 and 320 K increased up to 60 min. Thereafter, a slight increase in the uptake of MB was observed up to 120 min, after which equilibrium was attained. At 340 K, the biosorption of MB increased up to 120 min, after which equilibrium was reached. Increment in the temperature made MB to exhibit a dissociated form that decreased the rate at which it bound onto the functional moieties in the pores of TISW [29, 62].

The biosorption of Cd^{2+} onto TISW at 300 K increased up to 30 min, respectively, and >30 min of Cd^{2+} uptake culminated into equilibrium. For the biosorption of Pb^{2+} by TISW at 320 and 340 K, the uptake of Pb^{2+} increased up to 15 min, after which equilibrium was observed. The increase in the mass transfer of Pb^{2+} onto the functional moieties in the TISW pores was due to the fast diffusion of Pb^{2+} from the solute phase onto the sorbent [61, 62].

Equilibrium, kinetics and thermodynamics of CR, MB, Cd^{2+} and Pb^{2+} removal by TISW

To know the biosorption capacity of TISW for CR, MB, Cd^{2+} and Pb^{2+}, the experimental data were modelled with some equilibrium models. Langmuir isotherm fits the experimental data for the removal of CR, MB, Cd^{2+} and Pb^{2+} by TISW better than the Freundlich and Temkin isotherms. The correlation co-efficient values for the Langmuir isotherm were higher than those for Freundlich and Temkin isotherms. The saturation monolayer adsorption capacities, $q_{\max_L}$, of TISW for CR, MB, Cd^{2+} and Pb^{2+} were 85.47, 175.44, 12.58 and 52.91 mg g^{-1}, respectively (see Table 3). Lucidly, it is noteworthy to say that the homogeneous nature of TISW surface favoured the uptake of MB molecules more than the other pollutant ions of interest in this work. From Freundlich isotherm, it can be deduced that the values for the biosorption affinity, $1/n$, for the uptake of CR, MB, Cd^{2+} and Pb^{2+} onto TISW were

Table 4 Nonlinear equilibrium parameters for the removal of Methylene Blue, Congo Red, Cadmium and Lead onto *Terminalia ivorensis* seed waste

	MB − $q_{e\,(exp)}$	MB − $q_{e\,(model)}$	CR − $q_{e\,(exp)}$	CR − $q_{e\,(model)}$	Cd^{2+} − $q_{e\,(exp)}$	Cd^{2+} − $q_{e\,(model)}$	Pb^{2+} − $q_{e\,(exp)}$	Pb^{2+} − $q_{e\,(model)}$
Nonlinear Freundlich model								
Reduced χ^2	974.71	36.14	894.71	3.57E−5	403.34	0.34	32.15	0.68
Residual sum of squares	1949.41	72.27	1789.42	7.15E−5	806.68	0.68	111.87	1.36
Adjusted R^2	0.95	0.99	0.70	1.00	0.91	1.00	0.97	1.00
Nonlinear Langmuir model								
Reduced χ^2	479.73	0.21	948.07	2.99E−5	403.35	0.05	2251.11	0.01
Residual sum of squares	1939.41	0.43	9814.22	5.97E−5	818.20	0.11	651.93	0.01
Adjusted R^2	0.95	1.00	0.67	1.00	0.93	1.00	0.99	1.00
Nonlinear Temkin model								
Reduced χ^2	974.72	7.84E−5	849.17	0.01	403.34	0.53	757.62	1.60
Residual sum of squares	1949.41	1.57E−4	1798.14	0.01	608.86	1.06	223.50	3.21
Adjusted R^2	0.96	1.00	0.67	1.00	0.91	1.00	0.98	1.00

0.93, 2.41, 0.43 and 0.53, respectively. This suggests that the binding of MB onto TISW would be least favourable by heterogeneous surface, while the binding of Cd^{2+} onto TISW would be most favourable by heterogeneous surface ($0 < 1/n < 1$-favourable, $1/n > 1$-non favourable).

The nonlinear plots (Langmuir, Freundlich and Temkin isotherms) for the removal of CR, MB, Pb^{2+} and Cd^{2+} by TISW are shown in Fig. 6a–c. From these nonlinear isotherm plots, it was deduced that the equilibrium data better fit the nonlinear isotherms than the linear isotherms due to the higher correlation coefficient values (R^2 values) obtained for these plots, when compared with those obtained for linear isotherm plots. For the nonlinear isotherm plots, the reduced Chi square values (χ^2 values) and the residual sum of squares values indicated that Langmuir isotherm better fits the equilibrium data than Freundlich and Temkin isotherms (see Table 4).

The kinetics of biosorption gives a good idea of how the experimental timing controls the mechanism, chemical reaction and the bulk transfer of the solute ions onto the biosorbent surface. Table 5 indicates that pseudo-second-order kinetic equation gave better fits to the experimental data than pseudo-first-order kinetic equation for the removal of CR, MB, Cd^{2+} and Pb^{2+} by TISW. The correlation co-efficient values for pseudo-second-order kinetic equation were higher than those obtained for pseudo-first-order kinetic equation at the experimental temperatures. This suggests that the mechanism for the biosorption process is chemisorption. The pseudo-second-order rate constants, k_2, for the removal of CR, MB, Cd^{2+} and Pb^{2+} by TISW at 300–340 K were $k_2 \leq 0.417$ g mg^{-1} min^{-1}, while the pseudo-first-order rate constants, k_1, for the removal of CR, MB, Cd^{2+} and Pb^{2+} by TISW at 300–340 K were $k_1 \leq 0.026$ min^{-1}. The Weber–Morris intraparticle diffusion equation indicated that the plots did not pass through the origin, due to the fact that the values of the boundary film or the thickness of the boundary layer were $c \geq 0$ in all cases. This implies that intraparticle diffusion process was not the only rate controlling or limiting step for the biosorption process, but pore diffusion and film diffusion might have taken place in the rate controlling or limiting step [29, 63, 64].

The nonlinear plots (pseudo-first-order, pseudo-second-order and intraparticle diffusion equations) for the removal of CR, MB, Pb^{2+} and Cd^{2+} onto TISW are shown in Tables 6 and 7. It was deduced that the kinetic data better fit the nonlinear kinetic equation than the linear kinetic equations. This resulted from the fact that the correlation coefficient values (R^2 values) obtained for these plots were higher than those obtained for the linear kinetic equations. For the nonlinear kinetic plots, the reduced Chi square values (χ^2 values) and the residual sum of squares values suggested that pseudo-second-order equations gave better fit to the kinetic data when compared to pseudo-first-order and intraparticle diffusion equations. Figure 7a–c depicts the nonlinear kinetic plots for pseudo-first-order, pseudo-second-order and intraparticle diffusion equations for biosorbed CR, MB, Cd^{2+} and Pb^{2+} by TISW. But this work has shown that low-cost TISW demonstrated remediation potential for both toxic industrial dyestuffs and toxic metal ions. Hence, TISW has a wide array of applications for environmental remediation.

From thermodynamic standpoint (see Table 8), $+\Delta G°$ (kJ/mol) values increased from 6.53 to 7.40, 7.67 to 8.69, 23.87 to 27.05 and 13.31 to 15.09 as TISW biosorbed CR, MB, Cd^{2+} and Pb^{2+} from 300 to 340 K, respectively. The $\Delta H°$ (kJ/mol) values were −0.27, −0.40, +0.09 and +0.22 for the biosorption of CR, MB, Cd^{2+} and Pb^{2+} by TISW,

Table 5 Linear kinetic parameters for the removal of Methylene Blue, Congo Red, Cadmium and Lead onto *Terminalia ivorensis* seed waste

	Temperature (K)	PFOM			PSOM			WMID		
		k_1 (/min)	q_e (mg/g)	R^2	k_2(g/mg min)	q_e (mg/g)	R^2	k_{id} (g/mg $min^{1/2}$)	R^2	c
MB	300	0.026	0.974	0.806	0.011	12.920	0.997	0.081	0.880	11.283
	320	0.023	1.458	0.805	0.057	12.390	0.999	0.130	0.687	10.738
	340	0.019	1.734	0.694	0.085	11.420	0.999	0.106	0.849	10.076
CR	300	0.020	4.575	0.929	0.012	7.949	0.994	0.307	0.923	3.951
	320	0.022	2.557	0.764	0.046	7.868	0.999	0.021	0.511	5.003
	340	0.022	2.177	0.904	0.051	4.235	0.995	0.014	0.606	2.180
Cd(II)	300	0.011	0.679	0.952	0.417	11.710	1.000	0.029	0.964	11.915
	320	0.008	1.332	0.755	0.339	12.300	1.000	0.023	0.927	11.417
	340	0.021	0.556	0.712	0.303	12.240	1.000	0.005	0.508	11.560
Pb(II)	300	0.004	0.771	0.062	0.224	12.250	1.000	0.034	0.694	11.831
	320	0.011	1.178	0.805	0.142	11.600	1.000	0.087	0.951	10.976
	340	0.008	1.270	0.694	0.085	12.150	1.000	0.013	0.379	10.298

PFOM nonlinear pseudo-first-order model, *PSOM* nonlinear pseudo-second-order model, *WMID* Weber–Morris intraparticle diffusion model

respectively. The $-\Delta S°$ (J mol^{-1} K^{-1}) values for CR, MB, Cd^{2+} and Pb^{2+} biosorbed by TISW were 217.72, 255.71, 79.56 and 44.38, respectively. Table 8 depicts that the values of Gibb's free energy, ($\Delta G°$) for CR, MB, Cd^{2+} and Pb^{2+} biosorbed by TISW were non-spontaneous at all temperatures. The values of enthalpy change, ($\Delta H°$) for CR and MB biosorbed by TISW were exothermic, while those for Cd^{2+} and Pb^{2+} biosorbed by TISW were endothermic. The values of entropy change, ($\Delta S°$) for CR, MB, Cd^{2+} and Pb^{2+} biosorbed by TISW showed decreasing disorderliness or chaos of the biosorption process. Table 9 shows the adsorption capacities, q_{max_L}(mg/g) of some adsorbents for CR, MB, Cd^{2+} and Pb^{2+} used by researchers as reported in literature.

Desorption kinetics

Figure 8 shows that desorption of MB from MB-loaded TISW was maximum at 86.37% for 0.1 M HCl desorbent and also maximum at 79.77% for 0.1 M HNO_3 desorbent after 30 min. Similarly, desorption of CR from CR-loaded TISW was maximum at 92.73% for 0.1 M HCl desorbent and likewise maximum at 55.65% for 0.1 M HNO_3 desorbent after 30 min. The desorption kinetics of Cd^{2+}

Table 6 Nonlinear kinetic parameters for the removal of Methylene Blue and Congo Red onto *Terminalia ivorensis* seed waste

	MB						CR					
	300 K		320 K		340 K		300 K		320 K		340 K	
	$q_{t(exp)}$	$q_{t(model)}$	$q_{t(exp)}$	$q_{t(model)}$	$q_{t(exp)}$	$q_{t(model)}$	$q_{t(exp)}$	$q_{t(model)}$	$q_{t(exp)}$	$q_{t(model)}$	$q_{t(exp)}$	$q_{t(model)}$
PFOM												
Reduced χ^2	0.09	0.05	0.05	0.02	0.02	0.01	0.31	0.08	0.09	0.03	0.10	0.01
Residual sum of squares	0.56	0.31	0.31	0.12	0.10	0.01	1.87	0.46	1.12	0.21	0.62	0.08
Adjusted R^2	0.98	0.99	0.98	1.00	0.98	1.00	0.94	0.99	0.94	1.00	0.91	0.99
PSOM												
Reduced χ^2	1.25	0.76	0.05	0.04	0.03	0.02	0.31	0.19	0.19	0.11	0.10	0.05
Residual sum of squares	10.88	4.59	0.31	0.28	0.21	0.10	1.87	1.18	1.12	0.65	0.62	0.32
Adjusted R^2	0.93	0.97	0.98	1.00	0.98	1.00	0.94	0.98	0.94	0.98	0.91	0.98
WMID												
Reduced χ^2	20.83	4.70E−5	0.05	1.21E−4	0.02	8.08E−5	0.31	6.74E−4	0.19	3.06E−6	0.10	0.01
Residual sum of squares	1.22	2.82E−4	0.31	7.27E−4	0.10	4.85E−4	1.87	0.01	1.12	1.84E−5	0.62	0.05
Adjusted R^2	0.93	1.00	0.98	1.00	0.88	1.00	0.94	1.00	0.94	1.00	0.91	0.99

PFOM nonlinear pseudo-first-order model, *PSOM* nonlinear pseudo-second-order model, *WMID* Weber–Morris intraparticle diffusion model

Table 7 Nonlinear kinetic parameters for the removal of Cadmium and Lead onto *Terminalia ivorensis* seed waste

	Cd(II)						Pb(II)					
	300 K		320 K		340 K		300 K		320 K		340 K	
	$q_{t(exp)}$	$q_{t(model)}$	$q_{t(exp)}$	$q_{t(model)}$	$q_{t(exp)}$	$q_{t(model)}$	$q_{t(exp)}$	$q_{t(model)}$	$q_{t(exp)}$	$q_{t(model)}$	$q_{t(exp)}$	$q_{t(model)}$
PFOM												
Reduced χ^2	0.02	1.10E−4	0.01	1.25E−4	1.77	0.01	2.51	0.05	2.51	0.11	2.88	0.01
Residual sum of squares	0.01	6.60E−4	0.01	1.68E−4	2.81	0.02	3.23	0.09	6.55	0.53	6.79	0.03
Adjusted R^2	0.97	1.00	0.97	1.00	0.97	1.00	0.92	1.00	0.93	1.00	0.91	1.00
PSOM												
Reduced χ^2	0.02	6.22E−4	2.88	0.01	3.95	0.01	3.33	0.03	3.67	0.02	1.22	0.05
Residual sum of squares	0.25	0.03	31.65	0.02	5.99	0.03	12.56	0.07	6.48	0.35	8.15	0.07
Adjusted R^2	0.97	1.00	0.95	1.00	0.91	1.00	0.95	1.00	0.95	1.00	0.97	1.00
WMID												
Reduced χ^2	1.40	1.51E−6	0.02	6.13E−6	1.33	1.33	13.18	0.03	8.31	0.05	1.01	0.11
Residual sum of squares	8.40	4.25E−6	0.01	3.88E−5	7.82	0.03	5.15	0.05	7.07	1.03	7.24	0.85
Adjusted R^2	0.97	1.00	0.97	1.00	0.96	1.00	0.96	1.00	0.94	1.00	0.97	1.00

PFOM nonlinear pseudo-first-order model, *PSOM* nonlinear pseudo-second-order model, *WMID* Weber–Morris intraparticle diffusion model

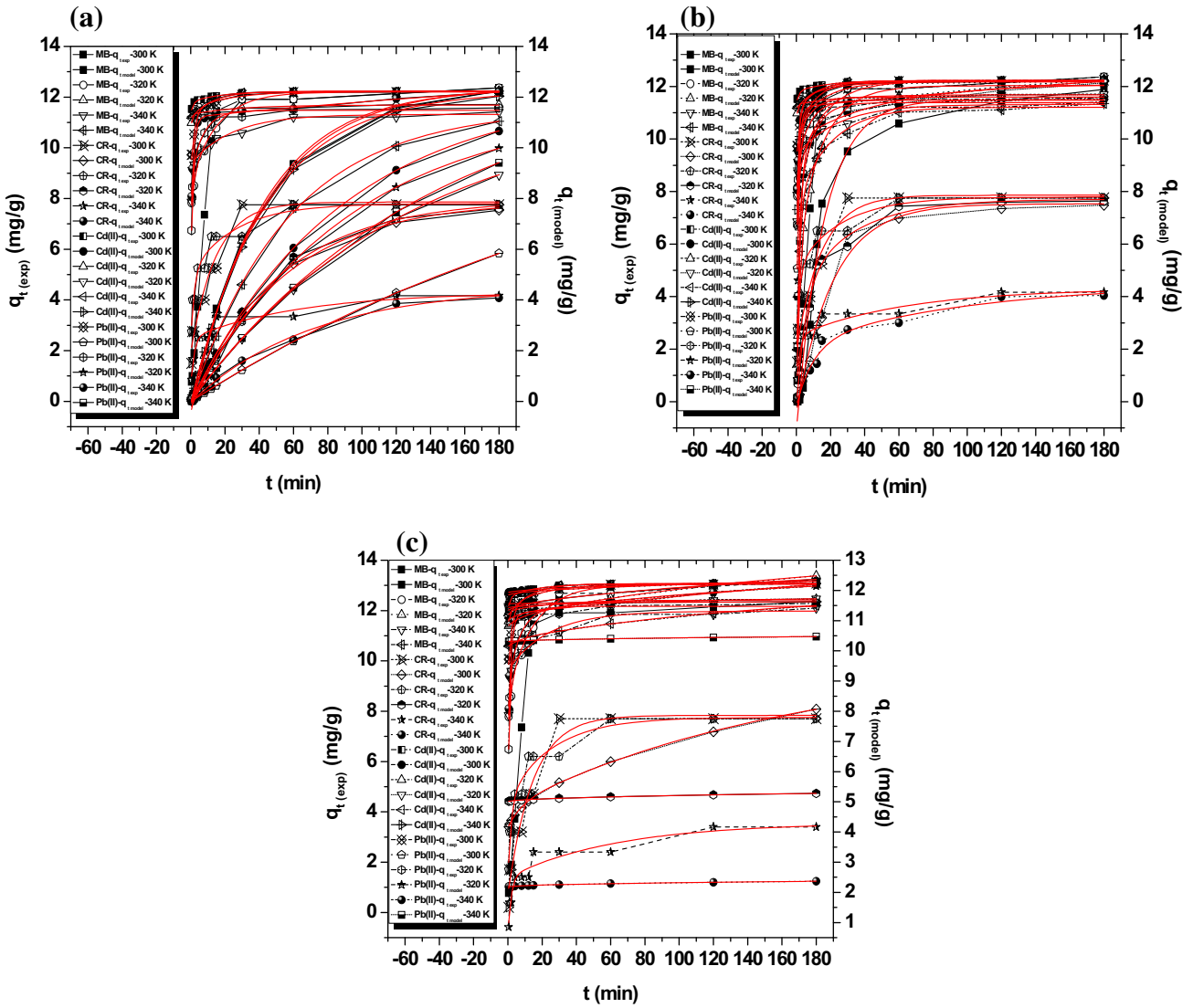

Fig. 7 **a** Nonlinear pseudo-first-order kinetic plots of Methylene Blue, Congo Red, Cadmium and Lead biosorbed by *Terminalia ivorensis* seed waste (temperature = 300–340 K; adsorbent dose = 25 mg; agitation speed = 200 rpm; initial metal ion concentration = 100 mg/L; agitation time = 0.5–180 min). **b** Nonlinear pseudo-second-order kinetic plots of Methylene Blue, Congo Red, Cadmium and Lead biosorbed by *Terminalia ivorensis* seed waste (temperature = 300–340 K; adsorbent dose = 25 mg; agitation speed = 200 rpm; initial metal ion concentration = 100 mg/L; agitation time = 0.5–180 min). **c** Nonlinear Weber–Morris intraparticle diffusion kinetic plots of Methylene Blue, Congo Red, Cadmium and Lead biosorbed by *Terminalia ivorensis* seed waste (temperature = 300–340 K; adsorbent dose = 25 mg; agitation speed = 200 rpm; initial metal ion concentration = 100 mg/L; agitation time = 0.5–180 min)

Table 8 Thermodynamic parameters for the removal of Methylene Blue, Congo Red, Cadmium and Lead onto *Terminalia ivorensis* seed waste at different temperatures

	$+\Delta G^{\circ}$ (kJ/mol)			ΔH° (kJ/mol)	$-\Delta S^{\circ}$ (J/mol/K)
	300 K	320 K	340 K		
TISW-CR	6.53	6.97	7.40	-0.27	217.72
TISW-MB	7.67	8.18	8.69	-0.40	255.71
TISW-Pb^{2+}	13.31	14.20	15.09	+0.22	44.38
TISW-Cd^{2+}	23.87	25.46	27.05	+0.09	79.56

Table 9 The adsorption capacities, q_{max_L} (mg/g) of some adsorbents used by researchers

Adsorbents	References	q_{max_L} (mg/g)			
		Cd^{2+}	Pb^{2+}	MB	CR
Eucalyptus seed waste	[9]	71.15			
Solanum melongena	[10]		71.42		
Peanut hull	[11]	6.00	30.00		
Corn cob	[12]	5.38			
Hazelnut shell	[13]	5.47	16.46		
Olive cake	[14]	65.40			
Mungbean husk	[15]	35.41			
Mango peel waste	[16]	68.92	99.05		
Orange waste biomass	[17]	41.58			
Scolymus hispanicus L.	[18]	54.05			
Chemically modified orange peel	[19]	13.70	73.53		
Nauclea diderrichii seed waste	[20]	6.30			
Zea mays seed chaff	[22]	121.95	384.62		
Graphene oxide/*Nauclea diderrichii* seed waste	[23]	7.54	7.94		
Parkia biglobosa biomass	[24]	157.98	94.25		
Papaya-clay combo	[25]			35.46	
Nano-titania/*Nauclea diderrichii* seed waste	[26]		7.49		
Pentaclethra macrophylla bark	[29]	43.76	348.43	251.26	157.23
Malacantha alnifolia bark	[29]	255.75	133.87	89.00	800.00
Cedrela odorata seed waste	[39]			111.88	128.84
Parkia biglobosa cellulosic extract	[40]			1498.42	266.67
TISW	This study	12.58	52.91	175.44	85.47

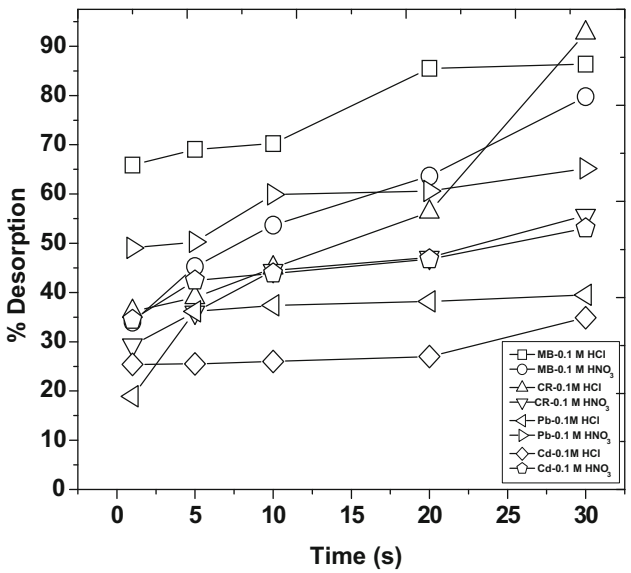

Fig. 8 Desorption kinetics of Methylene Blue, Congo Red, Cadmium and Lead loaded-*Terminalia ivorensis* seed waste using 0.1 M HCl and 0.1 M HNO_3 (adsorbent dose = 25 mg; agitation speed = 200 rpm; agitation time = 1–30 min; temperature = 300 K)

showed that the maximum of 34.89 and 53.01% of Cd^{2+} was desorbed from Cd^{2+} loaded TISW using 0.1 M HCl and 0.1 M HNO_3 desorbents, respectively, after 30 min. Also, the maximum of 39.5 and 65.16% of Pb^{2+} was desorbed from Pb^{2+} loaded TISW using 0.1 M HCl and 0.1 M HNO_3 desorbents, respectively, after 30 min. Conversely, desorption of CR and MB from TISW was kinetically faster than that of Cd^{2+} and Pb^{2+} from TISW. This desorption kinetics result reveals that TISW can be regenerated and reused for another cycle of biosorption.

Conclusion

For the first time, *Terminalia ivorensis* seed waste (TISW) demonstrated a good potential for the removal of CR, MB, Cd^{2+} and Pb^{2+}. Proximate analysis, bulk density, specific surface area, pH of point of zero charge, Fourier transform infra red spectroscopy, scanning electron microscopy, thermogravimetric/differential thermal analysis and energy dispersive analysis of X-ray were used to study the surface texture or morphology of TISW. The equilibrium data best fit the Langmuir isotherm, with a maximum Langmuir monolayer saturation adsorption capacity, q_{max_L} = 175.44 mg MB per g of TISW. The kinetic data best fit the pseudo-second-order equation for the removal of CR, MB, Cd^{2+} and Pb^{2+} onto TISW. This study revealed that TISW, a benign agricultural seed waste, could

be recommended as ubiquitous and cheap biological adsorbent for environmental remediation of toxic industrial dyestuffs and toxic metals.

Acknowledgements Dr. Martins O. Omorogie, who is currently a postdoctoral research fellow at Department of Chemistry, Vaal University of Technology (VUT), Vanderbijlpark, South Africa, appreciates the Department for providing TG/DTA (Perkin Elmer) for the surface textural characterisations of TISW. Dr. Martins O. Omorogie and Prof. Jonathan O. Babalola acknowledge the Department of Chemistry, University of Ibadan, Nigeria for the provision of FTIR (Perkin Elmer), FAAS (Buck Scientific 205) and UV/Visible Spectrophotometer (Cecil), which were used for various analyses.

References

1. Cabral JPS (2010) Water microbiology: Bacterial pathogens and water. Int J Environ Res Public Health 7:3657–3703
2. United Nations (2012) The millennium development goals report. United Nations, New York
3. Onda K, LoBuglio J, Bartram J (2012) Global access to safe water: accounting for water quality and the resulting impact on MDG progress. Int J Environ Res Public Health 9:880–894
4. Kandile NG, Mohamed HM, Mohamed MI (2015) New heterocycle modified chitosan adsorbent for metal ions (II) removal from aqueous systems. Int J Biol Macromol 72:110–116
5. Hameed BH, Ahamad AA (2009) Batch adsorption of methylene blue from aqueous solution by garlic peel, an agricultural waste biomass. J Hazard Mater 164:3115–3121
6. Saha B, Das S, Saikia J, Das G (2011) Preferential and enhanced adsorption of different dyes on iron oxide nanoparticles: a comparative study. J Phys Chem C 115:8024–8033
7. Pang H, Wang WQ, Yan ZZ, Zhang H, Li XX, Chen J, Zhang JS, Zhang B (2012) Porous $Mn_3[Co(CN)_6]_2.nH_2O$ nanocubes as a rapid organic dyes adsorption material. RSC Adv 2:9614–9618
8. Chen ZH, Zhang JN, Fu JW, Wang MH, Wang XZ, Han RP, Xu Q (2014) Adsorption of methylene blue onto poly(cyclotriphosphazene-co-4,4′-sulfonyldiphenol) nanotubes: kinetics, isotherm and thermodynamics analysis. J Hazard Mater 273:263–271
9. Kiruba UP, Senthil Kumar P, Prabhakaran C, Aditya V (2014) Characteristics of thermodynamic, isotherm, kinetic, mechanism and design equations for the analysis of adsorption in Cd(II) ions-surface modified Eucalyptus seeds system. J Taiwan Inst Chem 45:2957–2968
10. Yuvaraja G, Krishnaiah N, Subbaiah MV, Krishnaiah A (2014) Biosorption of Pb(II) from aqueous solution by *Solanum melongena* leaf powder as a low-cost biosorbent prepared from agricultural waste. Colloids Surf B 114:75–81
11. Brown P, Jefcoat IA, Parrish D, Gill S, Graham E (2002) Evaluation of the adsorptive capacity of peanut hull pellets for heavy metals in solution. Adv Environ Res 4:19–29
12. Leyva-Ramos CR, Bernal-Jacome LA, Acosta-Rodriguez I (2005) Adsorption of cadmium(II) from aqueous solution on natural and oxidized corn cob. Sep Purif Technol 45:41–49
13. Bulut Y, Tez Z (2007) Adsorption studies on ground shells of hazelnut and almond. J Hazard Mater 149:35–41
14. Anber ZA, Matouq MAD (2008) Batch adsorption of cadmium ions from aqueous solution by means of olive cake. J Hazard Mater 151:194–201
15. Saeed A, Iqbal M, Holl WH (2009) Kinetics, equilibrium and mechanism of Cd^{2+} removal from aqueous solution by mungbean husk. J Hazard Mater 168:1467–1475
16. Iqbal M, Saeed A, Zafar SI (2009) FTIR spectrophotometry, kinetics and adsorption isotherms modeling, ion exchange, and EDX analysis for understanding the mechanism of Cd^{2+} and Pb^{2+} removal by mango peel waste. J Hazard Mater 164:161–171
17. Marin ABP, Ortuno JF, Aguilar MI, Meseguer VF, Saez J, Llorens M (2010) Use of chemical modification to determine the binding of Cd(II), Zn(II) and Cr(III) ions by orange waste. Biochem Eng J 53:2–6
18. Barka N, Abdennouri M, Boussaoud A, Makhfouk M-EI (2010) Biosorption characteristics of cadmium(II) onto *Scolymus hispanicus L.* as low-cost natural biosorbent. Desalination 258:66–71
19. Lashee MR, Ammar NS, Ibrahim HS (2012) Adsorption/desorption of Cd(II), Cu(II) and Pb(II) using chemically modified orange peel: equilibrium and kinetic studies. Solid State Sci 14:202–210
20. Omorogie MO, Babalola JO, Unuabonah EI, Gong JR (2012) Kinetics and thermodynamics of heavy metal ions sequestration onto novel *Nauclea diderrichii* seed biomass. Bioresour Technol 118:576–579
21. Omorogie MO, Babalola JO, Unuabonah EI, Song W, Gong JR (2016) Efficient chromium abstraction from aqueous solution using a low-cost biosorbent: *Nauclea diderrichii* seed waste. J Saudi Chem Soc 20(1):49–57
22. Babalola JO, Omorogie MO, Babarinde AA, Unuabonah EI, Oninla VO (2016) Optimization of the biosorption of Cr^{3+}, Cd^{2+} and Pb^{2+} using new biowaste: *Zea mays* seed chaff. Environ Eng Manage J 15(7):1571–1580
23. Omorogie MO, Babalola JO, Unuabonah EI, Gong JR (2014) Solid phase extraction of hazardous metals from aqua system by nanoparticle-modified agrowaste composite adsorbents. J Environ Chem Eng 2(1):675–684
24. Omorogie MO, Babalola JO, Unuabonah EI, Gong JR (2014) Hybrid materials from agrowaste and nanoparticles: implications on the kinetics of the adsorption of inorganic pollutants. Environ Technol 35(5):611–619
25. Ogbodu RO, Omorogie MO, Unuabonah EI, Babalola JO (2015) Biosorption of heavy metals from aqueous solutions by *Parkia biglobosa* biomass: equilibrium, kinetics, and thermodynamic studies. Environ Prog Sustain Energy 34(6):1694–1704
26. Unuabonah EI, Adedapo AO, Nnamdi CO, Adewuyi A, Omorogie MO, Adebowale KO, Olu-Owolabi BI, Ofomaja AE, Taubert A (2015) Successful scale-up performance of a novel Papaya-clay combo adsorbent: up-flow adsorption of a basic dye. Desalin Water Treatment 56(2):536–551
27. Omorogie MO, Babalola JO, Unuabonah EI, Gong JR (2016) Clean technology approach for the competitive binding of toxic metal ions onto MnO_2 nano-bioextractant. Clean Techn Environ Policy 18(1):171–184
28. Omorogie MO, Babalola JO, Unuabonah EI, Gong JR (2015) New facile benign agrogenic-nanoscale titania material; Remediation potential for toxic inorganic cations. J Water Proc Eng 5(1):95–100
29. Babalola JO, Olowoyo JO, Durojaiye AO, Olatunde AM, Unuabonah EI, Omorogie MO (2016) Understanding the removal and regeneration potentials of biogenic wastes for toxic metals and organic dyes. J Taiwan Inst Chem Eng 58:490–499

30. Gupta VK, Srivastava SK, Mohan D, Sharma S (1998) Design parameters for fixed bed reactors of activated carbon developed from fertilizer waste material for the removal of some heavy metal ions. Waste Manage 17:517–522
31. Jain AK, Gupta VK, Bhatnagar A, Suhas A (2003) Comparative study of adsorbents prepared from industrial wastes for removal of dyes. Sep Sci Technol 38(2):463–481
32. Gupta VK, Mittal A, Kaur D, Malviya A, Mittal J (2009) Adsorption studies on the removal of colouring agent phenol red from wastewater using waste materials as adsorbents. J Colloid Interface Sci 337:345–354
33. Gupta VK, Mittal A, Kaur D, Malviya A, Mittal J (2009) Adsorptive removal of hazardous anionic dye 'congo red' from wastewater using waste materials and recovery by desorption. J Colloid Interface Sci 340:16–26
34. Gupta VK, Mittal A, Malviya A, Mittal J (2010) Decoloration treatment of a hazardous triaryl methane dye, light green SF (Yellowish) by waste material adsorbents. J Colloid Interface Sci 342:518–527
35. Khani H, Rofouei MK, Arab P, Gupta VK, Vafaei Z (2010) Multi-walled carbon nanotubes-ionic liquid-carbon paste electrode as a super selectivity sensor: application to potentiometric monitoring of mercury ion (II). J Hazard Mater 183:402–409
36. Gupta VK, Mittal A, Mittal J (2010) Removal and recovery of Chrysoidine Y from aqueous solutions by waste materials. J Colloid Interface Sci 344:497–507
37. Gupta VK, Jain R, Agarwal S, Shrivastava M (2011) Removal of the hazardous dye—Tartrazine by photodegradation on titanium dioxide surface. Mater Sci Eng C 31:1062–1067
38. Gupta VK, Agarwal S, Saleh TA (2011) Synthesis and characterization of alumina-coated carbon nanotubes and their application for lead removal. J Hazard Mater 185:17–23
39. Saleh TA, Gupta VK (2012) Photo-catalyzed degradation of hazardous dye methyl orange by use of a composite catalyst consisting of multiwalled carbon nanotubes and titanium dioxide. J. Colloids Interface Sci. 371:101–106
40. Gupta VK, Nayak A (2012) Cadmium removal and recovery from aqueous solutions by novel adsorbents prepared from orange peel and Fe_2O_3 nanoparticles. Chem Eng J 180:81–90
41. Gupta VK, Jain R, Mittal A, Agarwal S, Sikarwar S (2012) Photocatalytic degradation of toxic dye Amaranth on TiO_2/UV in aqueous suspensions. Mater Sci Eng C 32:12–17
42. Karthikeyan S, Gupta VK, Boopathy R, Titus A, Sekaran G (2012) A new approach for the degradation of aniline by mesoporous activated carbon as a heterogeneous catalyst: kinetic and spectroscopic studies. J Mol Liq 173:153–163
43. Saleh TA, Gupta VK (2012) Column with CNT/magnesium oxide composite for lead (II) removal from water. Environ Sci Pollut Res 19:1224–1228
44. Gupta VK, Ali I, Saleh TA, Nayak A, Agarwal S (2012) Chemical treatment technologies for waste-water recycling-an overview. RSC Adv 2:6380–6388
45. Gupta VK, Kumar R, Nayak A, Saleh TA, Barakat MA (2013) Adsorptive removal of dyes from aqueous solution onto carbon nanotubes: a review. Adv Colloid Interface Sci 193–194:24–34
46. Saleh TA, Gupta VK (2014) Processing methods, characteristics and adsorption behavior of tire derived carbons: a review. Adv Colloid Interface Sci 211:93–101
47. Gupta VK, Nayak Agarwal A (2015) Bioadsorbents for remediation of heavy metals: current status and their future prospects. Environ Eng Res 20:1–18
48. Mushtaq M, Bhatti HN, Iqbal M, Noreen S (2016) *Eriobotrya japonica* seed biocomposite efficiency for copper adsorption: isotherms, kinetics, thermodynamic and desorption studies. J Environ Manage 176:21–33
49. Tahir MA, Bhatti HN, Iqbal M (2016) Solar red and brittle blue direct dyes adsorption onto *Eucalyptus angophoroides* bark: equilibrium, kinetics and thermodynamic studies. J Environ Chem Eng 4:2431–2439
50. Rashid A, Bhatti HN, Iqbal M, Noreen S (2016) Fungal biomass composite with bentonite efficiency for nickel and zinc adsorption: a mechanistic study. Ecol Eng 91:459–471
51. Hanif MA, Bhatti HN (2015) Remediation of heavy metals using easily cultivable, fast growing, and highly accumulating white rot fungi from hazardous aqueous streams. Desal Water Treat 53:238–248
52. Zhao G, Li J, Ren X, Chen C, Wang X (2011) Few-layered graphene oxide nanosheets as superior sorbents for heavy metal ion pollution management. Environ Sci Technol 45(24):10454–10462
53. Yang S, Chen C, Chen Y, Li J, Wang D, Wang X, Hu W (2015) Competitive adsorption of Pb^{II}, Ni^{II}, and Sr^{II} ions on graphene oxides: a combined experimental and theoretical study. ChemPlusChem 80:480–484
54. Kennish MJ (1992) Ecology of estuaries: anthropogenic effects. CRC, Boca Raton
55. Ofomaja AE, Naidoo EB (2011) Biosorption of copper from aqueous solution by chemically activated pine cone: a kinetic study. Chem Eng J 175:260–270
56. Stumm W, Morgan JJ (1996) Aquatic chemistry, 3rd edn. Wiley, New York, pp 534–540
57. Sears GW (1956) Determination of specific surface area of colloidal silica by titration with sodium hydroxide. Anal Chem 28:1981–1983
58. Zhan Y, Luo X, Nie S, Huang Y, Tu X, Luo S (2011) Selective separation of Cu(II) from aqueous solution with a novel Cu(II) surface magnetic ion-imprinted polymer. Ind Eng Chem Res 50:6355–6361
59. Arshadi M, Faraji AR, Amiri MJ, Mehravar M, Gil A (2015) Removal of methyl orange on modified ostrich bone waste—a novel organic-inorganic biocomposite. J Col Interface Sci 446:11–23
60. Ho YS (1995) Adsorption of heavy metals from waste streams by peat, PhD Thesis, University of Birmingham, Birmingham, UK
61. Onal Y, Akmil-Basar C, Sarici-Ozdemir C (2007) Investigation kinetics mechanisms of adsorption malachite green onto activated carbon. J Hazard Mater 146:194–203
62. Vimonses V, Lei S, Jin B, Chow CWK, Saint C (2009) Kinetic study and equilibrium isotherm analysis of congo red adsorption by clay materials. Chem Eng J 148:354–364
63. Babalola JO, Koiki BA, Eniayewu Y, Salimonu A, Olowoyo A, Oninla VO, Alabi HA, Ofomaja AE, Omorogie MO (2016) Adsorption efficacy of *Cedrela odorata* seed waste for dyes: non linear fractal kinetics and non linear equilibrium studies. J Environ Chem Eng 4(3):3527–3536
64. Babalola JO, Bamidele TM, Adeniji EA, Odozi NW, Olatunde AM, Omorogie MO (2016) Adsorptive modelling of toxic cations and ionic dyes onto cellulosic extract. Model Earth Syst Environ 2(4):190–204